ELSEVIER

Cobalt supported on zirconia and sulfated zirconia I. FT-IR spectroscopic characterization of the NO_x species formed upon NO adsorption and NO/O_2 coadsorption

Margarita Kantcheva [*] and Ahmet S. Vakkasoglu

Department of Chemistry, Bilkent University, 06800 Bilkent, Ankara, Turkey

Abstract

Cobalt catalysts are prepared by impregnating zirconia and sulfated zirconia using an aqueous solution of cobalt(II) acetate. XRD results show that the catalysts with 5 wt% cobalt loading contain a small amount of Co_3O_4. Analysis of the FT-IR results on the adsorption of NO at room temperature reveals the formation of cobalt(II) mono- and dinitrosyls. It is shown that the nitrosyls formed on the sulfate-free catalyst with 5 wt% cobalt loading are unstable on prolonged contact with NO at room temperature due to the oxidation of adsorbed NO to NO_2^- (nitro) and NO_3^- species by cobalt(III) originating from the Co_3O_4 phase. This process does not occur in the case of the sulfated catalyst containing the same amount of cobalt, for which the existence of a Co_3O_4 phase is also detected. This experimental fact leads to the conclusion that the sulfate ions lower the reducibility of cobalt(III). Upon coadsorption of NO and O_2 at room temperature on the samples studied, various kinds of surface nitrates are observed differing in the modes of their coordination. In the case of CoO_x/SO_4^{2-}–ZrO_2 catalysts, part of the bidentate nitrates transform to NO_2^- (nitro) species after evacuation at 373 K. The nitro-nitrato species on the sulfated catalysts are characterized by a lower thermal stability than that of the nitrates on the CoO_x/ZrO_2 samples.
© 2004 Elsevier Inc. All rights reserved.

Keywords: Adsorption of NO and NO/O_2; In situ FT-IR; CoO_x/ZrO_2; CoO_x/ZrO_2–SO_4^{2-}

1. Introduction

The limited hydrothermal stability of zeolite-based catalysts for the selective catalytic reduction of NO_x with hydrocarbons (CH-SCR) is a serious obstacle to their industrial applications. Due to this problem, there is a renewed interest in the utilization of simple oxides with strong surface acidity, such as sulfated zirconia, as alternative supports [1–13]. Hamada et al. [14] first reported that sulfated TiO_2, ZrO_2, and Fe_2O_3 are active in the reduction of NO with propane. The performance of sulfated zirconia (SZ) in this reaction has been further improved by promotion with copper and gallium oxides [7]. Recent reports showed that in the reduction of NO with propene, sulfated zirconia containing copper [11] or cobalt [12] exhibits much greater activity and selectivity than the corresponding sulfate-free samples. It has been found that Pd/SZ [2–5,8], Pt–Pd/SZ [9,10], and

Co/SZ [13] can be used as effective catalysts for SCR of NO with methane in the presence of oxygen. The good catalytic performance in the CH-SCR of materials based on sulfated zirconia is related to the ability of this support to maintain the high dispersion of the active component of the catalyst, preventing the formation of oxide phases such as PdO, Co_3O_4, or CuO, which favor the complete oxidation of the reducer [3–5,11–13]. In addition, sulfate-modified zirconia has good hydrothermal stability [1,4] and catalysts based on this support do not undergo irreversible deactivation in wet streams [4–6,10] like the zeolite-based materials.

The modification of zirconia with SO_4^{2-} ions decreases the amount of adsorbed NO_x^- species relative to the sulfate-free support and lowers their thermal stability [15]. A possible analogous effect of sulfates could be expected in the case of cobalt supported on sulfated zirconia. In this study, by means of in situ FT-IR spectroscopy, we have characterized the surface NO_x species, obtained during the adsorption of NO and its coadsorption with oxygen on samples containing the same amount of cobalt (2.8 and 5 wt% nominal content)

supported on zirconia and sulfated zirconia (nominal content of 4.5 wt% SO_4^{2-} ions).

2. Experimental

2.1. Sample preparation

The preparation of the cobalt–zirconia samples involves three steps: (i) synthesis of amorphous hydrated zirconia by hydrolysis of $ZrCl_4$ (Merck, for synthesis) with a concentrated (25%) solution of ammonia according to the procedure described earlier [15]: (ii) the material obtained in step (i) was dried at 393 K for 12 h and impregnated by dosed amounts of cobalt(II) acetate solution in order to get a nominal cobalt content of 2.8 and 5 wt%, respectively (the amount of the hydrated zirconia was determined on the base of the weight loss after calcination for 2 h at 623 K and 2 h at 773 K); (iii) calcination of the impregnated materials for 2 h at 623 K and 2 h at 773 K.

The preparation of sulfated cobalt catalysts involves the following steps: (i) sulfatation of hydrated zirconia (that belongs to the same preparation batch used for the synthesis of the CoO_x/ZrO_2 materials) by an amount of $(NH_4)_2SO_4$ solution giving 4.5 wt% of nominal sulfate content (the amount of hydrated zirconia was determined from its weight loss after the calcination steps as described above); (ii) the amorphous sulfated material was dried at 373 K for 12 h and calcined for 2 h at 623 K and 2 h at 773 K; (iii) impregnation of the sulfated zirconia with aqueous solutions of cobalt(II) acetate ensuring 2.8 and 5 wt% nominal cobalt content, followed by drying at 373 K and two calcination steps at 623 and 773 K for 2 h each.

The cobalt content was determined by atomic absorption (Buck Scientific, Model 200A). The amount of sulfate ions was analyzed by extraction with 1 M NaOH, followed by precipitation of the sulfate ions as barium sulfate. The precipitate was dissolved in a standard EDTA solution and the excess of EDTA was backtitrated with a standard magnesium solution using solochrome as indicator. The analytical content of the sulfate ions in the sulfated zirconia was 3.9 wt% corresponding to 3.8 SO_4^{2-}/nm^2, i.e., about the theoretical monolayer of 4.0 SO_4^{2-}/nm^2 [16]. The sulfate content of the used catalysts remained at the level of the fresh samples.

The nominal and analytical content of the samples, the surface areas, concentrations of the active components, and the notations used are summarized in Table 1. The theoretical loading of cobalt that corresponds to the monolayer (3.5 Co/nm^2) was estimated using the fact that there are 7 Zr^{4+} ions/nm^2 on complete dehydroxylated monoclinic zirconia [17] and assuming two anchoring sites per one cobalt atom. According to Morterra et al. [18], at surface concentrations of sulfate ions equal or greater than the theoretical monolayer, all coordinative positions of the Zr^{4+} ions are saturated. This means that the surface concentration of

Table 1
Surface areas and loading of the samples studied[a]

Sample	BET surface area (m^2/g)	Co (wt%)	SO_4^{2-} (wt%)	Co/nm^2	SO_4^{2-}/nm^2
ZrO_2	67	–	–	–	–
SZ	158	–	4.5 (3.9)	–	3.8
2.8CoZ	79	2.8 (2.6)	–	4.0	–
5CoZ	93	5.0 (4.8)	–	7.7	–
2.8CoSZ	169	2.8 (2.7)	4.5 (3.9)	1.8	3.8
5CoSZ	178	5.3 (5.1)	4.5 (3.9)	3.3	3.8

[a] All materials are calcined for 2 h at 623 K and 2 h at 773 K. The numbers in parentheses correspond to the analytical content. The surface concentrations are determined using the analytical content.

the cobalt ions on the sulfated samples corresponding to the theoretical monolayer should be equal to 4.0 Co/nm^2. The data in Table 1 show that the cobalt loading in the cobalt–zirconia samples exceeds that of the theoretical monolayer, whereas for the sulfated catalysts the surface concentration of cobalt is below it.

2.2. Surface area measurements and X-ray diffraction

The BET surface areas of the samples (dehydrated at 523 K) were measured by nitrogen adsorption at 77 K using a MONOSORP apparatus from Quanto Chrome. XRD analysis was performed on a Rigaku Miniflex diffractometer with Ni-filtered Cu-K$_\alpha$ radiation under ambient conditions. The crystallographic phase composition was calculated using the method of Toraya et al. [19]. Crystallite sizes are calculated from the peak broadening of principal peaks with the Scherrer formula [20].

2.3. Infrared spectroscopy

The FT-IR spectra were recorded on a Bomem MB 102 FT-IR (Hartman & Braun) equipped with a liquid-nitrogen-cooled MCT detector at a resolution of 4 cm^{-1} (128 scans). An absorption IR cell allowed recording of the spectra at ambient temperature and catalyst activation at higher temperatures. The cell was connected to a vacuum/adsorption apparatus. Self-supporting disks (0.028 g/cm^2) were used for the FT-IR studies. These specimens were activated by heating for 1 h in vacuum and in oxygen (13.3 kPa, passed trough a trap cooled in liquid nitrogen) at 673 K followed by evacuation for 1 h at the same temperature. The spectra of the activated samples (taken at ambient temperature) were used as a background reference. The spectra of the samples that had been subjected to elevated temperatures were recorded after the IR cell had been cooled to room temperature. All of the spectra presented (except those in Fig. 2) were obtained by subtraction of the corresponding background reference.

The computer peak fittings were performed using the minimum number of peaks and fixed peak positions based on the original spectra. The sum of the squares of the devia-

tions between the experimental points and the fit values was less than 10^{-3}.

The purity of NO gas was 99.9% (Air Products).

3. Results and discussion

3.1. Structural characterization of the samples

Fig. 1 shows a representative X-ray diffraction pattern of the catalysts studied and supports used. The zirconia support is predominantly monoclinic (91%). The calcination of the hydrous sulfated zirconia does not lead to complete transformation of the monoclinic structure to tetragonal. The material obtained (sample SZ) contains a 33% monoclinic phase. Introduction of cobalt to the hydrated zirconia (catalysts 2.8CoZ and 5CoZ) converts the structure of the support from monoclinic to 100% tetragonal, whereas the impregnation with cobalt does not have a considerable effect on the phase composition of sulfated zirconia: the 2.8CoSZ and 5CoSZ catalysts are 70 and 67% tetragonal, respectively. The average crystallite sizes are 11 and 8 nm for the sulfated and unsulfated catalysts, respectively. The XRD patterns of the 5CoZ and 5CoSZ catalysts contain a weak
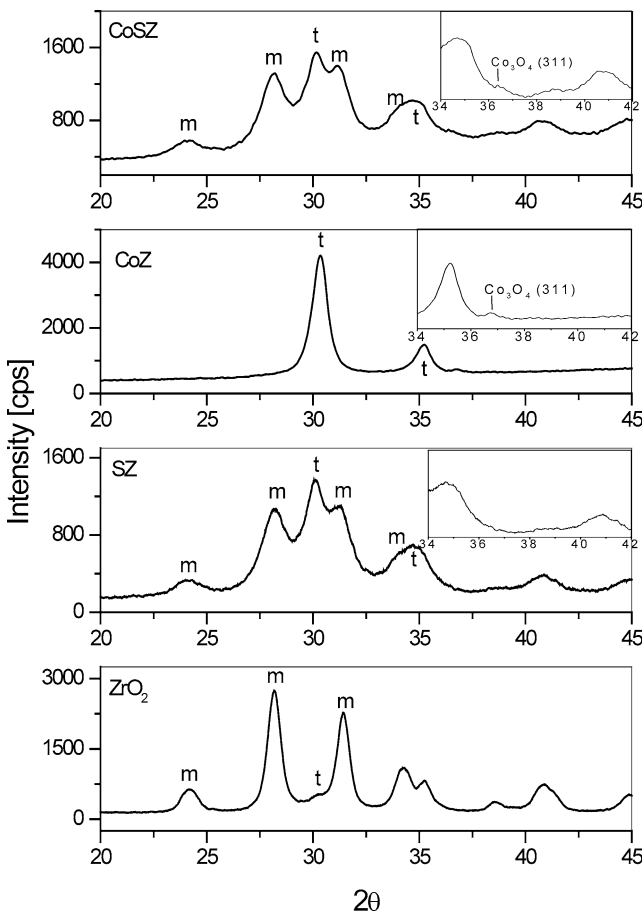
peak at $2\theta = 36.6$–$36.8°$ (see the insets in Fig. 1), which is attributed to the strongest (311) diffraction line of cubic Co_3O_4 [21,22]. It seems that in the case of the 5CoSZ catalyst this peak is broader due to the lower crystallinity of the sample.

Fig. 2 shows the FT-IR spectra of the activated catalysts together with the spectra of pure and sulfated (SZ) zirconia. The spectrum of the ZrO_2 support in the OH-stretching region displays a pair of sharp bands at 3771 and 3675 cm^{-1} assigned [15,23,24] to terminal (3771 cm^{-1}) and bridged (3675 cm^{-1}) hydroxyls coordinated to three Zr atoms. The broad band between 3600 and 3000 cm^{-1} is attributed to H-bonded hydroxyls.

The variation of the intensities of the surface hydroxyls of the cobalt-containing samples relative to those of the supports accounts for the participation of the corresponding Zr^{4+}–OH groups in the deposition of cobalt(II).

The complex band with a maximum at 1360 cm^{-1} and a shoulder at about 1388 cm^{-1} observed on the sulfated samples corresponds to the $\nu(S=O)$ vibration of highly covalent sulfates coordinated to Zr^{4+} ions, whereas the absorption in the 1200–870 cm^{-1} region is assigned to $\nu(S$–$O)$-stretching vibrations [25]. The shoulder at 1163 cm^{-1} observed in the spectra of the 2.8- and 5CoSZ samples reveals the presence of more ionic sulfates [26] attached to the cobalt sites. The occurrence of the transformation of covalent sulfates to more
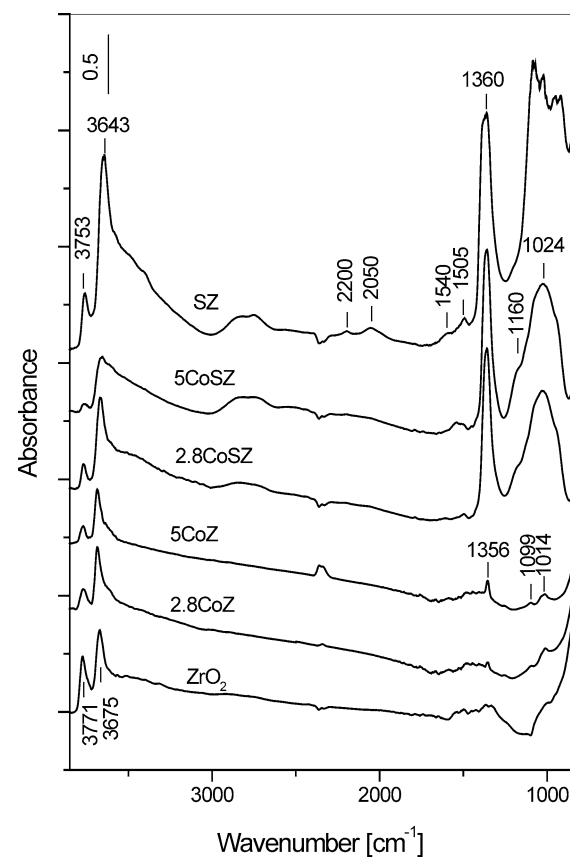

Fig. 1. Powder X-ray diffraction patterns of the ZrO_2, SZ, 5CoZ, and 5CoSZ samples (m, monoclinic; t, tetragonal).

Fig. 2. FT-IR spectra of the activated catalysts and supports used.

ionic structures is confirmed by the decrease in the intensity of the 1360 cm^{-1} band in the cobalt–sulfated zirconia catalysts relative to that in the SZ sample.

Sulfate-containing samples exhibit a broad absorption between 3000 and 2600 cm^{-1}. This absorption was previously assigned to the first overtones of the complex band with a maximum at 1360 cm^{-1} due to the ν(S=O) mode [15]. However, absorptions at 2970 and 2450 cm^{-1} corresponding to asymmetric and symmetric OH-stretching vibrations, respectively, have been observed in solid and liquid H_2SO_4 [27,28]. Based on this, we reinterpret the absorption between 3000 and 2600 cm^{-1} as ν(OH)-stretching vibrations of hydrogen sulfate species involved in intermolecular H bonding. The weak bands at 2200 and 2050 cm^{-1} detected in the case of sulfated zirconia are assigned to the first overtones of the ν(S–O) modes found between 1090 and 1000 cm^{-1}.

The bands between 1550 and 1400 cm^{-1}, detected with variable intensities for all of the samples studied, are assigned to split ν_3 modes of surface carbonates [23,29,30]. Such residual species are often observed on zirconia surfaces and cannot be removed by high-temperature activation of the catalyst [31]. The absorption at 2360 and 2335 cm^{-1} together with the sharp band at 1356 cm^{-1} observed on the 2.8- and 5CoZ samples is due to linearly adsorbed CO_2 [29,30]. The former pair of bands corresponds to a $\nu_3(CO_2)$-stretching vibration of CO_2 coordinated to two different Lewis acid sites, whereas the latter is due to the $\nu_1(CO_2)$ mode. The $\nu_1(CO_2)$ symmetric vibration is Raman active. However, due to lowering the symmetry of adsorbed CO_2, this band becomes IR active [29]. Most probably CO_2 appears as a product of the decomposition of the residual carbonates during the activation of the sample and adsorbs on the surface when the temperature is lowered. Bolis et al. [30] reported relatively stable CO_2 adsorbed on tetragonal zirconia resisting room-temperature evacuation. The contamination of the samples with carbonates could be related to the cobalt(II) acetate used as a precursor.

3.2. Adsorption of NO at room temperature on the CoO_x/ZrO_2 samples

The spectra of NO (1.07 kPa) adsorbed at room temperature on the 2.8CoZ sample for 7 and 60 min, respectively, contain strong bands at 1868 and 1781 cm^{-1} (Fig. 3A) typical of Co(II) nitrosyls [12,32–34]. The results of curve fitting of the spectrum taken after 60 min of NO adsorption (Fig. 3B) reveal the presence of two different cobalt(II) adsorption sites giving rise to mono- (ν(NO) at 1868 cm^{-1}) and dinitrosyls (ν_s(NO) at 1876 and ν_{as}(NO) at 1781 cm^{-1}). The dinitrosyl angle calculated using the integrated absorbances of the ν_{as}(NO) and ν_s(NO) bands is $111 \pm 1°$, which is close to those of cobalt(II) dinitrosyls in zeolites [35]. The intensities of the nitrosyl bands do not change upon prolonged contact with the NO. However, a noticeable increase in the absorption in the 3650–3000 cm^{-1} region

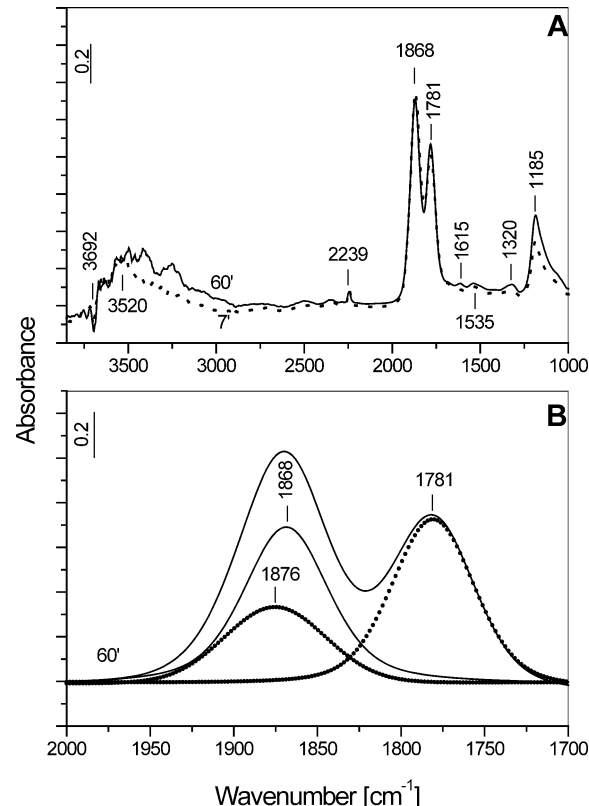Fig. 3. (A) FT-IR spectra of NO (1.07 kPa) adsorbed at room temperature on the 2.8CoZ catalyst for 7 and 60 min. The spectrum of the activated sample is used as a background reference. (B) Results of the curve-fitting procedure applied to the FT-IR spectrum in the 2000–1700 cm^{-1} region taken 60 min after the NO adsorption (1.07 kPa, room temperature) on the 2.8CoZ sample.

and in the intensity of the band at 1185 cm^{-1} is detected. The latter band was observed upon NO adsorption on pure zirconia [15] and was assigned to anionic nitrosyl, NO$^-$. Most probably this species interacts with the surface hydroxyls (negative band at 3692 cm^{-1}) leading to the appearance of a positive absorption in the 3550–3000 cm^{-1} region due to H-bonded OH groups. The weak bands at 1615, 1535, and 1320 cm^{-1} indicate the presence of a small amount of nitro-nitrate species. The sharp band at 2239 cm^{-1} is due to adsorbed N_2O [15].

Contrary to the 2.8CoZ sample, the increase in the time of NO adsorption causes a gradual decrease in the intensities of the cobalt(II) nitrosyl bands and a shift to higher frequencies (Fig. 4A). Simultaneously, the bands in the 1650–1000 cm^{-1} region grow, which is accompanied by the appearance of negative bands at 3770 and 3689 cm^{-1} due to altered OH groups (positive absorption in the 3600–3000 cm^{-1} region). The best curve fitting of the spectrum in the nitrosyl region taken after 6 min of NO exposure is obtained assuming the existence of two types of dinitrosyls and a mononitrosyl with a ν(NO)-stretching vibration superimposed to the ν_s(NO) modes of both $Co^{2+}(NO)_2$ species (Fig. 4B). The average dinitrosyl angles of both types of $Co^{2+}(NO)_2$ species, calculated using the integrated absorbances of the ν_{as}(NO) and
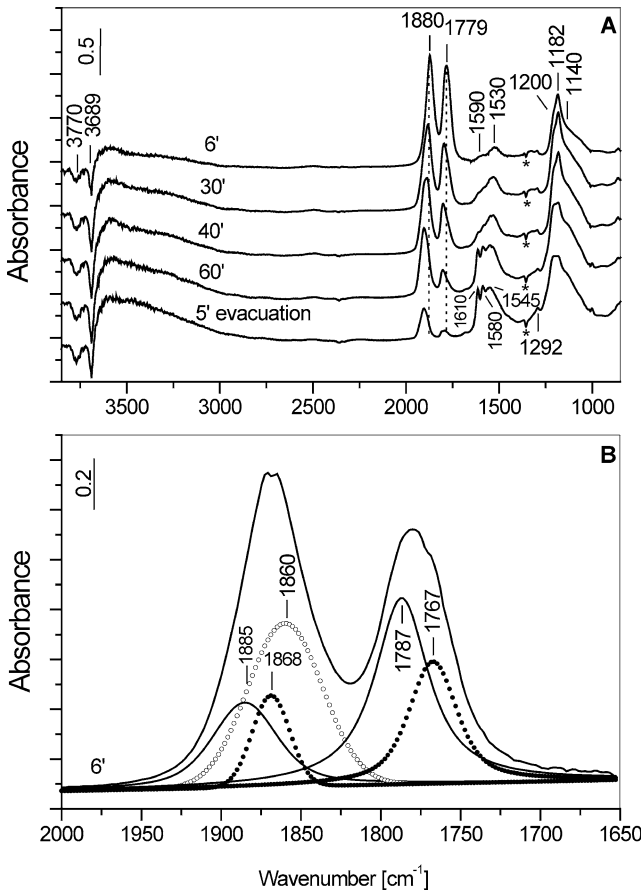
Fig. 4. (A) FT-IR spectra of NO (1.07 kPa) adsorbed at room temperature on the 5CoZ catalyst for various times. The spectrum of the activated sample is used as a background reference. The negative band at 1335 cm^{-1} marked by an asterisk is due to nitrate species adsorbed on the window of the IR cell. (B) Results of the curve-fitting procedure applied to the FT-IR spectrum in the 2000–1650 cm^{-1} region taken 6 min after the NO adsorption (1.07 kPa, room temperature) on the 5CoZ sample.

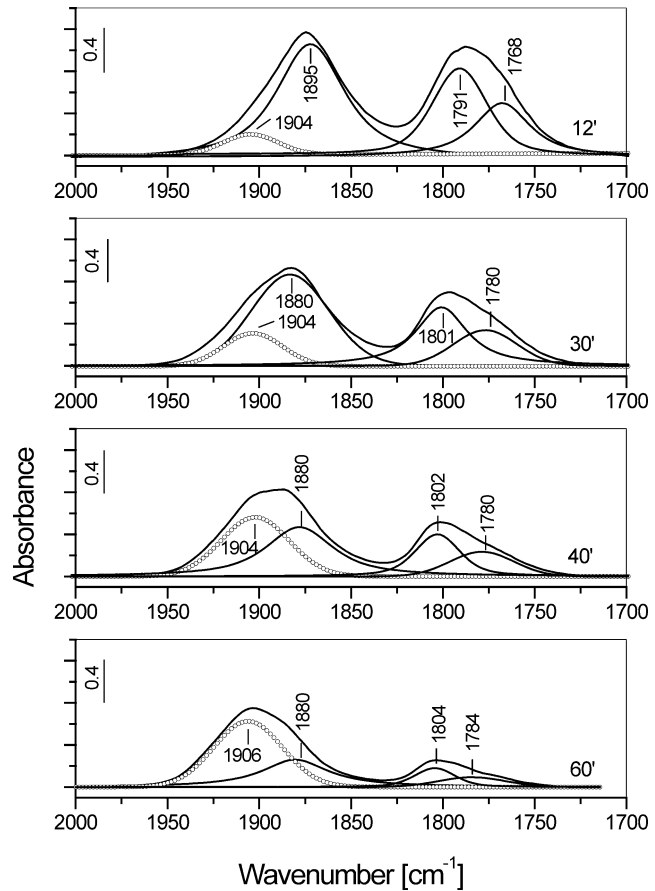
Fig. 5. Results of the curve-fitting procedure applied to the FT-IR spectra in the 2000–1700 cm^{-1} region taken at various times of NO adsorption (1.07 kPa, room temperature) on the 5CoZ sample.

ν_s(NO) bands at various times of NO adsorption, are 109 ± 1 and $111 \pm 1°$, respectively. These results indicate that the increase in the cobalt loading leads to an increase in the heterogeneity of the cobalt(II) sites.

In the low-frequency region, a strong and complex band at 1182 cm^{-1} with shoulders at 1200 and 1140 cm^{-1} develops (Fig. 4A). The subtraction spectra (not included) show that the bands at 1200 and 1140 cm^{-1} behave synchronously. These bands are ascribed to the ν_{as}(NO$_2$) and ν_s(NO$_2$)-stretching vibrations, respectively, of bidentate nitrito, NO$_2^-$, species [36]. The absorption at 1182 cm^{-1} (as in the case of the 2.8CoZ sample) is assigned to the ν(NO)-stretching mode of NO$^-$ species.

The results of the curve fitting of the spectra taken in the period from 6 to 60 min (Fig. 5) show that the intensities of the bands due to the nitrosyl species decrease with simultaneous growth of a band at 1906–1904 cm^{-1}. For the sake of simplicity, the band at 1895–1800 cm^{-1} represents the sum of the ν(NO) and ν_s(NO) modes of the cobalt(II) mono- and dinitrosyls, respectively.

Fig. 6 displays the plots of the integrated absorbances of the bands corresponding to the ν_{as}(NO) modes of the dinitrosyl species and the band at 1545–1530 cm^{-1} versus the integrated absorbance of the band at 1906–1904 cm^{-1} at various times of NO absorption. The linear relationships observed suggest that the species characterized by the absorptions at 1906–1904 and 1545–1530 cm^{-1} are produced at the expense of the cobalt(II) dinitrosyls. It can be assumed that the adsorbed NO is oxidized by cobalt(III) sites originating from the Co$_3$O$_4$ phase. The band at 1545–1530 cm^{-1} falls in a region typical of bridging nitro species [36]. The following reaction scheme can be proposed in which Co^{2+}(NO)$_2$ species are involved with formation of bridged nitro species:
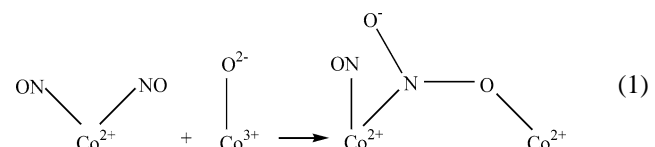
The band at 1904–1906 cm^{-1} is assigned to the ν(NO)-stretching vibration of the nitrosyl-nitro complex of the type ON–Co^{2+}–NO$_2^-$.
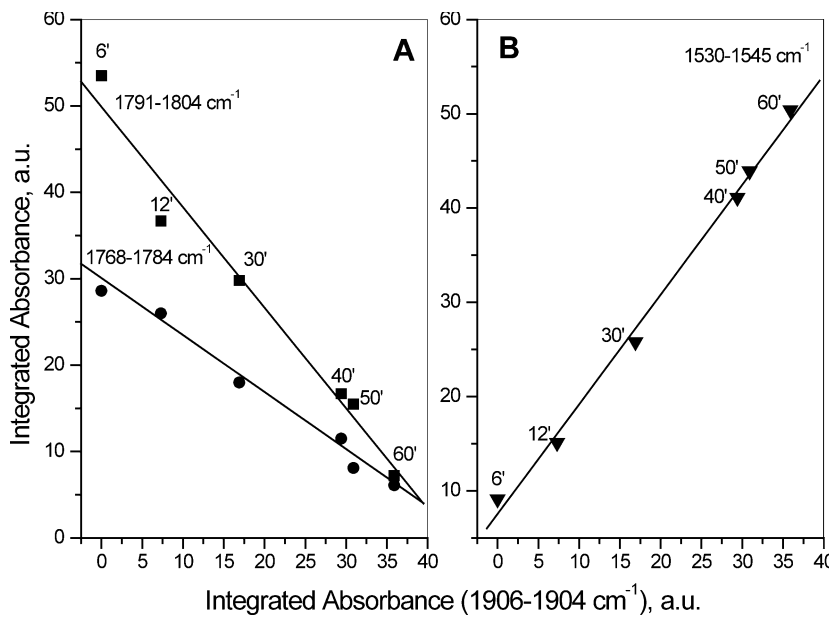
Fig. 6. (A) Correlation between the integrated absorbances of the bands due to the ν_{as}(NO) modes of the cobalt(II) dinitrosyls and the integrated absorbance of the ν(NO) band of the ON–Co^{2+}–NO$_2^-$ species produced during NO adsorption (1.07 kPa, room temperature) at various times on sample 5CoZ. (B) Correlation between the integrated absorbances of the bands assigned to the ν_{as}(NO$_2$) and ν(NO) modes of the ON–Co^{2+}–NO$_2^-$ species produced during NO adsorption (1.07 kPa, room temperature) at various times on sample 5CoZ.
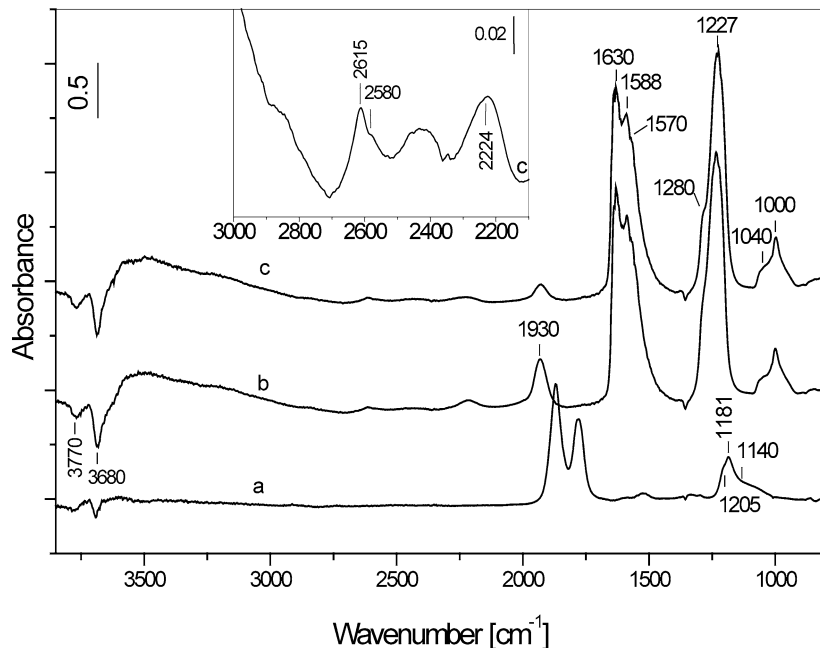

Fig. 7. FT-IR spectra of NO (0.67 kPa) (a) adsorbed on sample 5CoZ at room temperature for 5 min, (b) after subsequent introduction of O$_2$ (0.67 kPa) for 30 min, and (c) after evacuation for 15 min at room temperature. The spectrum of the activated sample is used as a background reference.

It should be pointed out that no linear relationship has been observed when the integrated absorbances of the bands at 1610 and 1580 cm^{-1} (see Fig. 4A) have been plotted versus the integrated absorbance of the band at 1906–1904 cm^{-1}. The former two bands are assigned to surface nitrates produced by oxidation of the cobalt(II) mononitrosyls.

3.3. Coadsorption of NO and O$_2$ on the CoO$_x$/ZrO$_2$ samples and thermal stability of the NO$_x$ species produced

Fig. 7 shows the spectra of the 5CoZ sample obtained upon adsorption of 0.67 kPa of NO for 5 min (spectrum a), followed by the addition of 0.67 kPa of O$_2$ to the IR cell for 30 min (spectrum b). The spectrum of adsorbed NO changes

completely in the presence of oxygen. The bands due to cobalt(II) nitrosyls disappear and absorption at 1930 cm^{-1} is observed instead. In the nitro-nitrato region, after the evacuation of the gas phase (spectrum c), three sets of bands with poorly resolved maxima at 1630, 1588, and 1570; 1280 and 1227; and 1041 and 1000 cm^{-1} are formed. The band at 1140 cm^{-1} (due to the $\nu_s(NO_2)$ mode of the bidentate nitrito species) disappears. Most probably the absorption due to NO$^-$ ions is not present in the spectrum as well, because it is known that in NO/O$_2$ atmosphere, the anionic nitrosyl converts into nitrato species [15]. The weak bands between 2900 and 2100 cm^{-1} (see the inset in Fig. 7) correspond to overtone and combination modes of the fundamental nitrate bands. It has been shown [15] that this spectral region can be used for structural identification of bridged and bidentate nitrate species. The broad absorption between 2900 and 2700 cm^{-1} reveals the presence of bridged nitrates whereas the band at 2615 cm^{-1} with a broad shoulder at 2580 cm^{-1} indicates that at least two kinds of bidentate nitrates are formed.

The band at 1930 cm^{-1} is assigned to the $\nu(NO)$-stretching mode of NO adsorbed on Co^{2+} ion, which has nitrate species in its coordination sphere, i.e., to the complex (ON)–Co^{2+}–(NO$_3^-$). This assignment is consistent with the observed stability of the band at 1930 cm^{-1} on evacuation, indicating that the strength of the adsorption site is increased by the electron-withdrawing NO$_3^-$ group. Since the NO$_3^-$ ions are more electronegative than the NO$_2^-$ species, the $\nu(NO)$ stretching in the case of the mixed nitrosyl-nitrato complex of Co^{2+} is at a higher frequency (1930 cm^{-1}) than that observed in the nitrosyl-nitro species (1904–1906 cm^{-1}).

The additional increase in the intensities of the negative bands at 3770 and 3680 cm^{-1} after the admission of oxygen accompanied by the appearance of a broad band in the $\nu(OH)$-stretching region of the H-bonded OH groups (Fig. 7, spectrum b) suggests that the terminal and bridged Zr^{4+}–OH groups are either affected by the nearby NO$_x$ species or involved in the formation of the nitrate species as proposed for zirconia [15] and titania [37–39]. The latter process leads to the appearance of adsorbed water.

Room-temperature evacuation does not affect the nitrate bands. However, heating the sample at 373 K (Fig. 8) results in the disappearance of the nitrosyl band at 1930 cm^{-1} and a decrease in the intensities of the nitrate bands. The bridged nitrates (1640–1620, 1220, and 1060 cm^{-1}) disappear after heating at 573 K. This conclusion is confirmed by the fact that the weak bands at 1990 and 1910 cm^{-1} due to the combination modes of bridged nitrates [15] are not observed after the above treatment. The bidentate nitrates (three kinds at 1615–1605, 1229, and 997; 1590, 1229, and 1040; and 1550, 1229, and 1040 cm^{-1}) display the highest thermal stability—they disappear after heating at 623 K. The negative bands at 3772 and 3686 cm^{-1} observed in the latter spectrum indicate that the Zr^{4+}–OH groups are not restored and they are lost during the high-temperature vacuum treat-
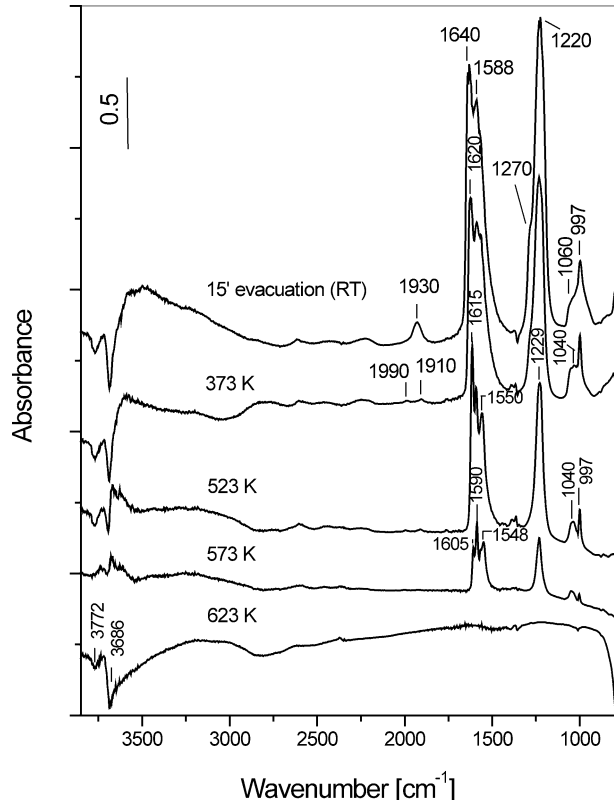

Fig. 8. FT-IR spectra obtained after heating of the catalyst 5CoZ containing adsorbed NO$_x$ species for 15 min in vacuum. The spectra are recorded after cooling of the IR cell to room temperature. Spectrum [15′ evacuation (RT)] is obtained after adsorption of NO/O$_2$ mixture (1.33 kPa, NO:O$_2$ = 1:1) for 30 min followed by evacuation for 15 min at room temperature. The spectrum of the activated sample is used as a background reference.

ment. This behavior indicates that the Zr^{4+}–OH groups are involved in the formation of the nitrate species. It should be pointed out that the nitrate species formed on the 2.8CoZ sample display similar thermal stability.

The absorption bands observed on the cobalt–zirconia samples after exposure to either NO or NO/O$_2$ mixture are summarized in Table 2.

3.4. Adsorption of NO at room temperature on the CoO$_x$/SO$_4^{2-}$–ZrO$_2$ samples

Contrary to the cobalt–zirconia samples the adsorption of NO (1.07 kPa, room temperature) on both 2.8CoSZ and 5CoSZ catalysts is time dependent (Figs. 9A and 9B). The spectrum of the 5CoSZ sample taken 6 min after the introduction of NO into the IR cell contains two strong bands in the nitrosyl region positioned at 1889 and 1800 cm^{-1}. The band at 1889 cm^{-1} has a high-frequency shoulder (Fig. 9C). The results of the curve fitting show that there are two different cobalt adsorption sites giving rise to mono- and dinitrosyls. The synchronous behavior of the bands at 1875 and 1796 cm^{-1} detected upon prolonged contact of the sample with NO (see below) allows us to assign them to $\nu_s(NO)$ and $\nu_{as}(NO)$ modes of Co^{2+}(NO)$_2$ species. The calculated

Table 2
Assignment of the FT-IR bands observed during adsorption of 0.67 kPa NO and its coadsorption with O_2 (NO:O_2 = 1:1) at room temperature on the 2.8- and 5CoZ samples

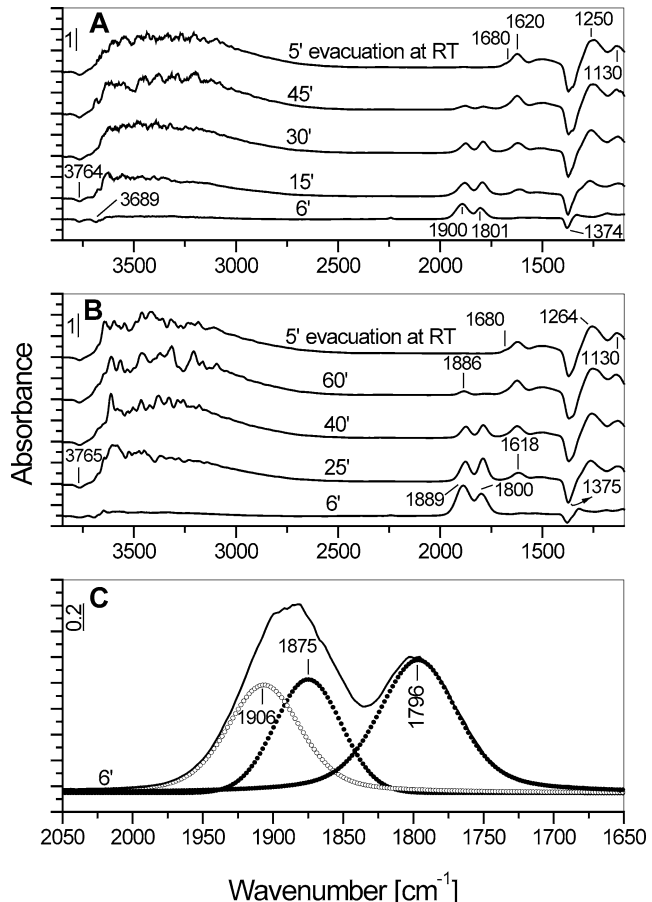| NO_x species	Band positions (cm^{-1})	Modes
ON–Co^{2+}–NO_3^-	1930	ν(NO)
ON–Co^{2+}–NO_2^-	1906–1904	ν(NO)
Co^{2+}(NO)$_2$	1885, 1787	ν_s(NO), ν_{as}(NO)
	1868, 1767	
Co^{2+}–NO	1860	ν(NO)
NO_2^- (bridging nitro)	1545–1530	ν_{as}(NO$_2$)
NO_2^- (bidentate nitrito)	1200, 1140	ν_{as}(NO$_2$), ν_s(NO$_2$)
NO^-	1182	ν(NO)
H_2O (adsorbed)	3660–3000,	ν(OH),
	1610–1590	δ(H$_2$O)
NO_3^- (bridged)	1640–1620	ν(N=O)
	1220, 1060	ν_{as}(NO$_2$), ν_s(NO$_2$)
	2900–2700	ν(N=O) + ν_{as}(NO$_2$)
	2224	ν_{as}(NO$_2$) + ν_s(NO$_2$)
	1990, 1910	ν_s(NO$_2$) + δ(NO$_2$)
NO_3^- (bidentate)	1615–1550	ν(N=O)
	1229	ν_{as}(NO$_2$)
	1040, 997	ν_s(NO$_2$)
	2615–2580	ν(N=O) + ν_s(NO$_2$)
	2420	$2\nu_{as}$(NO$_2$)
	2224	ν_{as}(NO$_2$) + ν_s(NO$_2$)
NO_3^- (monodentate)	1580, 1540	ν_{as}(NO$_2$)
	1292, 1270	ν_s(NO$_2$)

Fig. 9. (A) FT-IR spectra of NO (1.07 kPa) adsorbed at room temperature on the 2.8CoSZ (A) and 5CoSZ catalysts (B) for various times. The spectra of the activated samples are used as a background reference. (C) Results of the curve-fitting procedure applied to the FT-IR spectrum in the 2050–1650 cm^{-1} region taken 6 min after the NO adsorption (1.07 kPa, room temperature) on the 5CoSZ sample.

average dinitrosyl angle is $100 \pm 1°$, which is smaller than that of the dinitrosyls formed on the sulfate-free sample. This result is in good agreement with the value reported by Pietrogiacomi et al. [12]. Obviously, the geometry of the cobalt(II) dinitrosyl species is affected by the presence of sulfate ions. The absorption band at 1906 cm^{-1} falls in the spectral region typical of NO coordinated on strong Lewis acid sites. Therefore, we assign this band to the ν(NO) mode of Co^{2+}–NO species that have sulfate groups in the vicinity.

The behavior of the species observed upon prolonged contact of NO (1.07 kPa) at room temperature with the activated 2.8CoSZ and 5CoSZ samples (Figs. 9A and 9B) is similar to that described earlier for the sulfated zirconia [15]. The bands at 1680 and 1620–1618 cm^{-1} that grow with time, together with the absorption in the 3600–3000 cm^{-1}, have been assigned [15] to adsorbed cis-HNO$_2$ and H$_2$O. The fact that adsorbed water and nitrous acid are detected on both 2.8- and 5CoSZ samples implies that the analogous process of disproportionation of NO with the participation of surface hydroxyls as observed on the sulfated zirconia takes place. This process should lead also to the formation of NO$^-$ species. However, as proposed for the sulfated zirconia [15], the anionic nitrosyl is not stable in the presence of sulfate groups. The water produced causes (i) transformation of the sulfate groups from covalent polydentate (negative band at 1375 cm^{-1}) to more ionic bidentate species of C_{2v} symme-

try (positive bands at 1264–1250 and 1150–1130 cm^{-1} [15]) and (ii) displacement of the adsorbed NO. The latter conclusion is supported by the observed linear correlation between the integrated absorbances of the δ(H$_2$O) band and the bands due to the ν(NO) and ν_{as}(NO) modes of cobalt(II) mono- and dinitrosyls, respectively. Fig. 10 illustrates this relationship for the 5CoSZ sample.

Fig. 11 shows that in the case of the 5CoSZ sample, the least stable are the cobalt(II) mononitrosyls. The dinitrosyl bands at 1878 and 1795 cm^{-1} start to lose intensity after 25 min and disappear almost completely after 60 min. The band at 1888 cm^{-1} observed in the latter spectrum is assigned to the ν(NO) mode of mixed ON–Co^{2+}–OH$_2$ complexes.

3.5. Coadsorption of NO and O_2 on the CoO_x/SO_4^{2-}–ZrO_2 samples and thermal stability of the NO_x species produced

The spectra of the NO/O_2 (1.34 kPa, NO:O_2 = 1:1) adsorbed at room temperature on the 2.8CoSZ and 5CoSZ

samples are practically the same. Fig. 12 shows the spectra of the 5CoSZ sample obtained upon adsorption of NO (0.67 kPa) at room temperature followed by addition of O_2 (0.67 kPa). After 30 min, the gas phase was evacuated for 15 min at room temperature and the spectrum was recorded (spectrum a). The negative bands at 3768 and 3672 cm^{-1} observed in the ν(OH)-stretching region and the appearance of a broad absorption with maximum at 3200 cm^{-1}
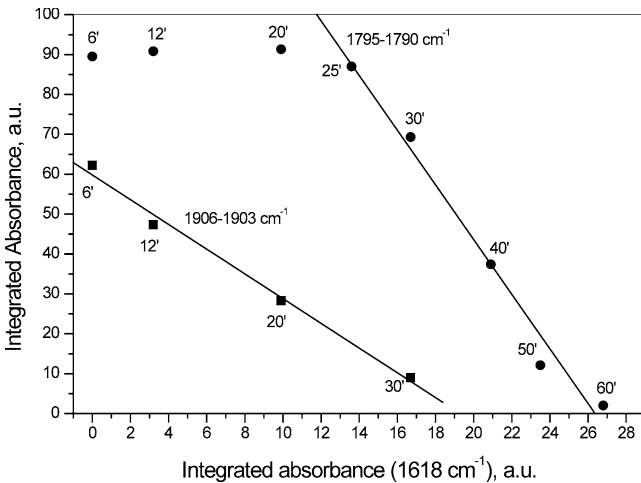

Fig. 10. Correlation between the integrated absorbances of the bands due to the ν(NO) and ν_{as}(NO) modes of the cobalt(III) mono- and cobalt(II) dinitrosyls and the integrated absorbance of the δ(H$_2$O) band at 1618 cm^{-1} produced during NO adsorption (1.07 kPa, room temperature) at various times on sample 5CoSZ.
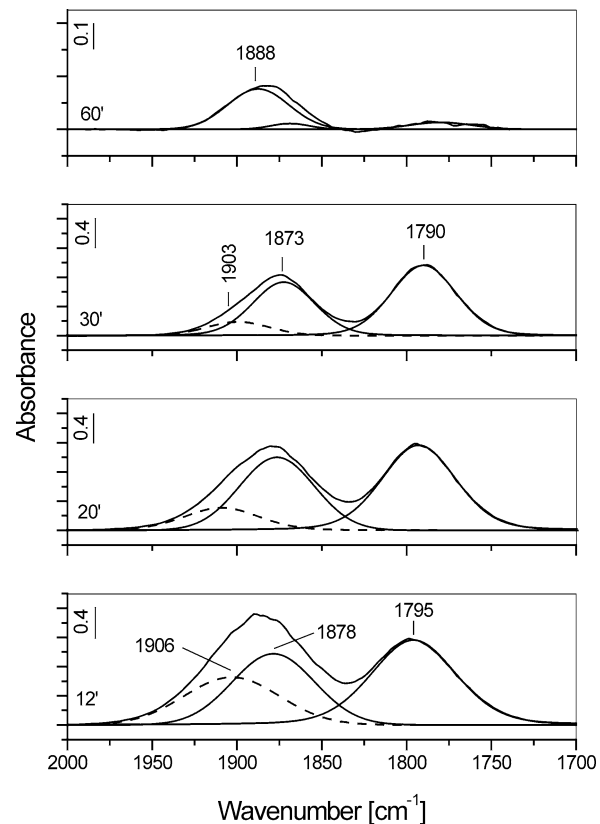

Fig. 11. Results of the curve-fitting procedure applied to the FT-IR spectra in the 2000–1700 cm^{-1} region taken at various times of NO adsorption (1.07 kPa, room temperature) on the 5CoSZ sample.
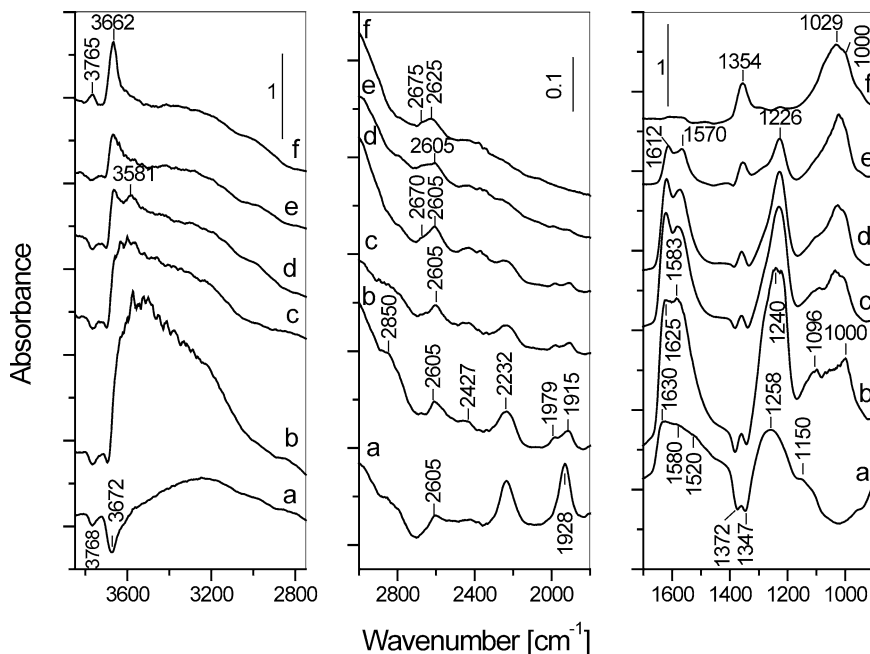

Fig. 12. FT-IR spectra obtained after heating of the catalyst 5CoSZ containing adsorbed NO$_x$ species for 15 min in vacuum at: (b) 373 K, (c) 423 K, (d) 473 K, (e) 523 K, and (f) 573 K. The spectra are recorded after cooling of the IR cell to room temperature. Spectrum (a) is obtained after adsorption of NO/O$_2$ mixture (1.33 kPa, NO:O$_2$ = 1:1) for 30 min followed by evacuation for 15 min at room temperature. The spectrum of the activated sample is used as a background reference.

suggest that in this case the surface OH groups are also either involved in the formation or perturbed by the adsorbed NO_x. The poorly resolved band with maximum at 1630 cm^{-1} and shoulders at approximately 1580 and 1520–1480 cm^{-1} can be attributed to various types of surface nitrates. The formation of bridged NO_3^- species is confirmed by the presence of a weak band in the combination nitrate region between 2900 and 2800 cm^{-1} [15]. The existence of bidentate NO_3^- species is evident by the absorption at 2605 cm^{-1} [15]. The unresolved intense absorption at 1258 cm^{-1} is attributed to the $\nu_{as}(NO_2)$ modes of the surface nitrates with a contribution from the perturbed sulfate groups (negative bands at 1372 and 1347 cm^{-1}). In agreement with the results on NO/O_2 adsorption on the 5CoZ sample, the band at 1928 cm^{-1} is assigned to mixed nitrosyl-nitrato complex.

Evacuation at 373 K for 15 min (spectrum b) causes a strong increase in the intensities of the bands in the ν(OH)-stretching and nitro-nitrato regions. The enhancement of the absorption in the ν(OH)-stretching region can be explained assuming, that surface hydroxyls are involved in the formation of nitrate species during the room-temperature NO/O_2 adsorption. This process leads to the formation of adsorbed water molecules that can undergo dissociation upon dynamic evacuation at 373 K leading to partial restoration of the consumed hydroxyls at 3672 cm^{-1} and appearance of H-bonded OH groups (strong band with maximum at 3560–3500 cm^{-1}). At the same time, the amount of the altered sulfate groups decreases considerably, which is evident by the reduced intensities of the negative bands at 1372 and 1347 cm^{-1}. This experimental fact indicates that the perturbation of the sulfate groups, observed during the room temperature NO/O_2 adsorption, is caused mainly by the water molecules evolved and the effect from the adsorbed NO_x species is less significant. Based on these considerations, the band at approximately 1150 cm^{-1} (Fig. 12, spectrum a) is assigned to water-perturbed sulfate groups.

In order to understand the reason for the drastic changes observed in the spectrum in the nitro–nitrato region (Fig. 12, spectrum b), analysis of the combination and fundamental nitrate bands has been performed (not reported for the sake of brevity). It is concluded that upon dynamic evacuation at 373 K, bridged nitro species are formed at the expense of some of the bidentate nitrates. A similar transformation of bidentate nitrates upon evacuation at elevated temperature to bridged nitro species has been observed in the case of zirconia-supported copper(II) catalyst [36]. The nitro species give rise to the strong band at 1583 cm^{-1} due to the $\nu_{as}(NO_2)$ mode (Fig. 12, spectrum b). The corresponding $\nu_s(NO_2)$ mode should fall between 1260 and 1180 cm^{-1} [36]. Indeed, strong enhancement in the absorption in this region is observed as well. The nitro species can appear during NO/O_2 coadsorption at room temperature, but their concentration increases significantly after evacuation at 373 K.

Table 3
Assignment of the FT-IR bands observed during adsorption of 0.67 kPa NO and its coadsorption with O_2 (NO:O_2 = 1:1) at room temperature on the 2.8- and 5CoSZ samples

NO_x species	Band positions (cm^{-1})	Modes
ON–Co^{2+}–NO$_3^-$	1928	ν(NO)
ON–Co^{2+}–OH$_2$	1888	ν(NO)
Co^{2+}–NO	1906–1903	ν(NO)
Co^{2+}(NO)$_2$	1878–1873, 1795–1790	ν_s(NO), ν_{as}(NO)
cis-HNO$_2$	1680	ν(N=O)
NO$_2^-$ (bridging nitro)	1583–1570	ν_{as}(NO$_2$)
H$_2$O (adsorbed)	3600–3000, 1618	ν(OH), δ(H$_2$O)
NO$_3^-$ (bridged)	1630–1625	ν(N=O)
	1240, 1100–1096	ν_{as}(NO$_2$), ν_s(NO$_2$)
	2900–2800	ν(N=O) + ν_{as}(NO$_2$)
	2232	ν_{as}(NO$_2$) + ν_s(NO$_2$)
	1979, 1915	ν_s(NO$_2$) + δ(NO$_2$)
NO$_3^-$ (bidentate)	1612	ν(N=O)
	1226, 1096	ν_{as}(NO$_2$), ν_s(NO$_2$)
	2605	ν(N=O) + ν_s(NO$_2$)
	2427	$2\nu_{as}$(NO$_2$)
	2232	ν_{as}(NO$_2$) + ν_s(NO$_2$)
NO$_3^-$ (monodentate)	1520–1480	ν_{as}(NO$_2$)

The bands in the combination region between 3000 and 1800 cm^{-1} and the absorption at 1620–1612, 1580–1570, and 1240–1226 cm^{-1} in the fundamental region lose their intensities on dynamic evacuation in the 423–523 K temperature range (Fig. 12, spectra c to e) and after the treatment at 573 K (spectrum f), they disappear almost completely. At the same time, a band at 1354 cm^{-1} together with the complex absorption with maximum at 1029 cm^{-1} starts to grow (Fig. 12, spectra c to f). This parallels the decrease in the intensity of the positive band due to H-bonded OH groups and that of the negative bands of the perturbed sulfate ions. Therefore, the band at 1354 cm^{-1} and the complex absorption at 1029 cm^{-1} with a shoulder at 1000 cm^{-1} are assigned to the ν(S=O) and ν(S–O) modes of restored sulfate groups, respectively. The latter have localization on the zirconia surface that differs from that of the original SO_4^{2-} species. Most probably, the restored sulfate groups are protonated, i.e., H$_x$SO$_4$ (x = 1 or 2). This gives rise to the sharp bands at 3662 and 3581 cm^{-1} corresponding to more acidic, isolated OH groups (Fig. 12, spectra d to f). The increase in the intensity of the band at 1354 cm^{-1} is accompanied by the appearance of a high-frequency shoulder at approximately 2670–2675 cm^{-1} to the nitrate combination band at 2605 cm^{-1}. Analogous to the interpretation of the absorption in the 2900–2700 cm^{-1} region proposed for the activated sulfated samples (see Fig. 2), the bands at 2675 and 2625 cm^{-1} (Fig. 12, spectrum f) are attributed to ν(OH)-stretching vibration of restored HSO$_4^-$ species involved in intermolecular H bonding.

Table 3 summarizes the assignment of the absorption bands observed during NO and NO/O$_2$ adsorption on the 2.8- and 5CoSZ samples.

4. Summary

Increasing the time of NO adsorption on the 5CoZ and 5CoSZ samples leads to a decrease in the intensities of the nitrosyl bands. However, the catalysts differ substantially in the reasons causing this decrease. According to the XRD data, a small amount of Co$_3$O$_4$ is detected in both samples. The Co^{3+} ions in the 5CoZ sample are able to oxidize the NO adsorbed on cobalt(II) to NO$_2^-$ (nitro) and NO$_3^-$ species at room temperature. This process does not occur in the case of the 5CoSZ catalyst. The decrease in the intensities of the nitrosyl bands is associated with the replacement of coordinated NO by water molecules produced by a surface reaction during the adsorption of NO. This conclusion is supported by the identical behavior of the 2.8CoSZ catalyst observed upon prolonged contact with NO. Formation of aggregated cobalt ions in this sample (with lower cobalt loading) could be excluded because the modification of the support with sulfate ions increases the dispersion. These experimental facts lead to the conclusion that the reducibility of cobalt(III) is lowered in the presence of sulfate ions and no oxidation of the NO adsorbed on the 5CoSZ sample takes place at room temperature.

In contrast to the 2.8CoSZ sample, the intensities of the cobalt(II) nitrosyl bands of the 2.8CoZ sample do not change with the time of NO exposure. This behavior supports the conclusion that the presence of the Co$_3$O$_4$ phase causes oxidation of the NO adsorbed on the sample with higher cobalt loading (5CoZ). However, it contradicts the reasonable expectation for the 2.8CoZ sample that if the adsorption of NO occurs through disproportionation, an analogous displacement of the coordinated NO by the water molecules produced in this process should take place. It is difficult to propose an unambiguous explanation about the different behavior of the sulfate-free and sulfate-modified samples with the same cobalt loading (2.8 wt%) in NO atmosphere. It is possible that during the NO adsorption, different processes of formation of the surface NO$_x$ species operate, depending on the presence or absence of sulfate ions. For example, the NO$^-$ species on the sulfate-free sample can appear as a result of NO adsorption on a single oxygen vacancy, whereas in the case of the sulfate-modified sample disproportionation of NO with the surface hydroxyls takes place leading to water formation. It should be pointed out that in the case of monoclinic zirconia the adsorption of NO has been proven to occur through disproportion involving the Zr^{4+}–OH groups by using deuterioxylated sample [15]. It can be proposed that this process prevails for the sulfated cobalt samples as well, which are mixtures of monoclinic and tetragonal phases and it does not take place in the case of the tetragonal cobalt–zirconia samples.

5. Conclusions

The structure of catalysts obtained by the impregnation of zirconia and sulfated zirconia with aqueous solutions of cobalt(II) acetate has been studied by means of XRD and FT-IR spectroscopy. According to XRD, the catalysts with 5 wt% cobalt loading contain some amount of Co$_3$O$_4$. The application of sulfated zirconia as a support results in a decrease in the average crystallite size (as compared to the sulfate-free samples) and better dispersion of the cobalt ions. In the presence of cobalt ions part of the original sulfate groups transforms from covalent to more ionic structures attached to cobalt sites.

The adsorption of NO on the 5 wt% CoO$_x$/ZrO$_2$ at room temperature results in the formation of cobalt(II) nitrosyls. The nitrosyls are unstable upon prolonged contact with NO due to the oxidation of adsorbed NO to NO$_2^-$ (nitro) and NO$_3^-$ species by cobalt(III) originating from the Co$_3$O$_4$ phase. This process does not occur in the case of the sulfated catalyst with the same cobalt content despite the presence of a Co$_3$O$_4$ phase. This experimental fact leads to the conclusion that the sulfate ions lower the reducibility of cobalt(III).

Upon coadsorption of NO and O$_2$ at room temperature on the samples studied, various kinds of surface nitrates are observed differing in the modes of their coordination. In the case of CoO$_x$/SO$_4^{2-}$–ZrO$_2$ catalysts, part of the bidentate nitrates and probably cobalt nitrosyls transform to NO$_2^-$ (nitro) species after evacuation at 373 K. The nitro-nitrato species on the sulfated catalysts are characterized by a lower thermal stability than that of the nitrates on the CoO$_x$/ZrO$_2$ samples.

References

[1] F.S. Feely, M. Deeba, R.J. Farrauto, G. Beri, A. Haynes, Appl. Catal. B 6 (1995) 79.
[2] C.J. Loughran, D.E. Resasco, Appl. Catal. B 7 (1995) 113.
[3] A. Ali, W. Alvarez, C.J. Loughran, D.E. Resasco, Appl. Catal. B 14 (1997) 13.
[4] Y.H. Chin, A. Pisanu, L. Serventi, W.E. Alvarez, D.E. Resasco, Catal. Today 54 (1999) 419.
[5] Y.H. Chin, W.E. Alvarez, D.E. Resasco, Catal. Today 62 (2000) 159.
[6] F. Figueras, B. Coq, E. Ensuque, D. Tachon, G. Delahay, Catal. Today 42 (1998) 117.
[7] J. Pasel, V. Speer, C. Albrecht, F. Richter, H. Papp, Appl. Catal. B 25 (2000) 105.
[8] H. Ohtsuka, Appl. Catal. B 33 (2001) 325.
[9] H. Ohtsuka, T. Tabata, Appl. Catal. B 29 (2001) 177.
[10] H. Ohtsuka, T. Tabata, T. Hirano, Appl. Catal. B 28 (2000) L73.
[11] V. Indovina, D. Pietrogiacomi, M.C. Campa, Appl. Catal. B 39 (2002) 115.
[12] D. Pietrogiacomi, M.C. Campa, S. Tuti, V. Indovina, Appl. Catal. B 41 (2003) 301.

[13] N. Li, A. Wang, J. Tang, X. Wang, D. Liang, T. Zhang, Appl. Catal. B 43 (2003) 195.

[14] H. Hamada, Y. Kintaichi, M. Tabata, M. Sasaki, T. Ito, Chem. Lett. (1991) 2179.

[15] M. Kantcheva, E.Z. Ciftlikli, J. Phys. Chem. B 106 (2002) 3941.

[16] C. Morterra, G. Cerrato, Phys. Chem. Chem. Phys. 1 (1999) 2825.

[17] V. Bolis, C. Morterra, M. Volante, L. Orio, B. Fubini, Langmuir 6 (1990) 695.

[18] C. Morterra, G. Cerrato, S.D. Ciero, Appl. Surf. Sci. 126 (1998) 107.

[19] H. Toraya, M. Yashimura, S. Somiya, J. Am. Ceram. Soc. 67 (1984) C119.

[20] M.P. Klug, L.E. Alexander, X-ray Diffraction Procedure for Polycrystalline and Amorphous Materials, Wiley, New York, 1974, p. 634.

[21] B. Jongsomjit, J. Panpranot, J.G. Goodwin Jr., J. Catal. 204 (2001) 98.

[22] S. Kaliaguine, A. Van Neste, V. Szabo, J.E. Gallot, M. Bassir, R. Muzychuk, Appl. Catal. A 209 (2001) 345.

[23] K.T. Jung, A.T. Bell, J. Mol. Catal. A 163 (2000) 27.

[24] G. Cerrato, S. Bordiga, S. Barbera, C. Morterra, Appl. Surf. Sci. 115 (1997) 53.

[25] C. Morterra, G. Cerrato, F. Pinna, M. Signoretto, J. Phys. Chem. 98 (1994) 12373.

[26] E. Laperdix, A. Sahibed-dine, G. Costentin, O. Saur, M. Bensitel, C. Nédez, A.B. Mohamed Saad, J.C. Lavalley, Appl. Catal. B 26 (2000) 71.

[27] G.E. Walrafen, D.M. Dodd, Trans. Faraday Soc. 57 (1961) 1286.

[28] P.A. Giguere, R. Savoie, J. Am. Chem. Soc. 85 (1963) 287.

[29] G. Busca, V. Lorenzelli, Mater. Chem. 7 (1982) 89.

[30] V. Bolis, G. Magnacca, G. Cerrato, C. Morterra, Top. Catal. 19 (2002) 259.

[31] C. Morterra, E. Giamello, G. Cerrato, G. Centi, S. Parathoner, J. Catal. 179 (1998) 111.

[32] X. Wang, H.Y. Chen, W.M.H. Sachtler, J. Catal. 197 (2001) 281.

[33] B. Djonev, B. Tsyntsarski, D. Klissurski, K. Hadjiivanov, J. Chem. Soc., Faraday Trans. 93 (1997) 4055.

[34] B. Tsyntsarski, V. Avreyska, H. Kolev, Ts. Marinova, D. Klissurski, K. Hadjiivanov, J. Mol. Catal. A 193 (2003) 139.

[35] Y. Li, T.S. Slager, J.N. Armor, J. Catal. 150 (1994) 388.

[36] M. Kantcheva, Appl. Catal. B 42 (2003) 89.

[37] M. Kantcheva, J. Catal. 204 (2001) 479.

[38] M.M. Kantcheva, V.P. Bushev, K.I. Hadjiivanov, J. Chem. Soc., Faraday Trans. 88 (1992) 3087.

[39] K. Hadjiivanov, V. Bushev, M. Kantcheva, D. Klissurski, Langmuir 10 (1994) 464.